



VICTORIA UNIVERSITY
MELBOURNE AUSTRALIA

*Detecting and attributing nonlinear anthropogenic
regional warming in southeastern Australia*

This is the Published version of the following publication

Jones, Roger (2012) Detecting and attributing nonlinear anthropogenic regional warming in southeastern Australia. *Journal of Geophysical Research*, 117 (D4). ISSN 0148-0227

The publisher's official version can be found at
<http://onlinelibrary.wiley.com/doi/10.1029/2011JD016328/pdf>
Note that access to this version may require subscription.

Downloaded from VU Research Repository <https://vuir.vu.edu.au/23209/>

Detecting and attributing nonlinear anthropogenic regional warming in southeastern Australia

Roger N. Jones¹

Received 31 May 2011; revised 9 December 2011; accepted 14 December 2011; published 23 February 2012.

[1] Nonlinear anthropogenic warming is detected and attributed as a series of step changes in observed and simulated climate for southeastern Australia (SEA). A stationary period of 1910–1967 and non-stationary period of 1968–2010 was established using statistically significant step-changes ($pH_0 < 0.01$) in the relationship between observed minimum (T_{\min}) and maximum (T_{\max}) temperature (0.6°C in 1968) and T_{\max} and rainfall (P ; 0.7°C in 1997). Regressions between these pairings during stationary conditions were used to determine how T_{\min} and T_{\max} would have evolved under non-stationary conditions. Assuming these relationships remain constant, the resulting residuals were attributed to anthropogenic regional warming. This warming was initiated as step changes in 1968 for T_{\min} (0.7°C) and 1973 for T_{\max} (0.5°C), coinciding with step changes in zonal (24–44°S) and southern hemisphere mean air temperatures (T_{av}). A step change in 1997 in T_{\max} (0.8°C) coincided with a statistically significant step change in global mean air temperature of 0.3°C. This analysis was repeated using regionally averaged output from eleven climate model simulations. Regional warming in all models commenced with step changes in T_{\min} ranging from 0.4 to 0.7°C between 1964 and 2003. T_{\max} underwent step changes ranging from 0.7 to 1.1°C simultaneously or within several decades. Further step changes, combined with rising trends, were simulated under increasing radiative forcing to 2100. This highlights limitations in the current use of the signal-to-noise model that considers anthropogenic climate change as a monotonic curve. The identification of multiple step changes in a changing climate provides important information for planning adaptation.

Citation: Jones, R. N. (2012), Detecting and attributing nonlinear anthropogenic regional warming in southeastern Australia, *J. Geophys. Res.*, 117, D04105, doi:10.1029/2011JD016328.

1. Introduction

[2] The issue of detecting and attributing climate change is considered to be a signal-to-noise problem [Hasselmann, 1979; Hulme and Mearns, 2001; Murphy *et al.*, 2009]. Santer *et al.* [2011] describe it thus: “The warming signal arising from slow, human caused changes in atmospheric concentrations of greenhouse gases is embedded in the background ‘noise’ of natural climate variability.” The main statistical model used to analyze and communicate climate change applies lines of best fit that largely remove this noise. The anthropogenic warming signal is assumed to change smoothly, with natural variability expressed as noise around that signal [e.g., Swanson *et al.*, 2009]. However, evidence of rapid climate change is a feature of past climates [Herweijer *et al.*, 2007; Mayewski *et al.*, 2004; Wanner *et al.*, 2008];

and the emergent properties of complex system dynamics provide the potential for abrupt changes in the future [e.g., Schneider, 2004].

[3] The main focus of detection and attribution studies is assessing whether climate has changed and attributing that change. The signal-to-noise model, however, also influences how climate information is analyzed and communicated for impacts and adaptation studies [Christidis *et al.*, 2012; Hawkins and Sutton, 2011; Hulme and Mearns, 2001; Murphy *et al.*, 2009]. The image of a gradually changing climate leads to adaptation being widely considered as a series of regular adjustments to such changes [e.g., Evans, 2009], despite extensive warnings this may not be case [Dessai *et al.*, 2009; Jones, 2010a; MacCracken *et al.*, 2008].

[4] Direct attribution involves detection of a significant change in a variable of interest. Observed changes in that variable are then compared with expected changes due to external forcing typically derived from modeling approaches [Hegerl *et al.*, 2010]. This method assumes that stationarity in control models runs adequately represents real-world stationarity. The null value theorem, where externally forced changes are compared against a control case(s) forced by internal variability, is then applied to show that observations

¹Centre for Strategic Economic Studies, Victoria University, Melbourne, Victoria, Australia.

are consistent with perturbed model runs. Statistical significance is obtained through the likelihood of observations matching control conditions [Stott *et al.*, 2010]. The application of such methods to Australian temperatures attributes a clear anthropogenic influence in the second half of the 20th century [CSIRO and BoM, 2007; Karoly and Braganza, 2005a].

[5] Regional climate change signals are also assumed to be linear with respect to mean global warming, allowing pattern scaling [Mitchell, 2003; Santer *et al.*, 1990]. Most regional climate change scenarios and projections are based on scaled regional changes to mean annual temperature, rainfall and other variables [IPCC-TGICA, 2007; Whetton *et al.*, 2005]. The most recent climate projections for Australia are based on this principle [CSIRO and BoM, 2007]. These projections form an envelope of uncertainty that opens up trumpet-like into the future. Decadal variability is acknowledged but is assumed to be independent of that signal.

[6] Since 1996, mean rainfall and temperature in southeastern Australia (SEA) have shifted beyond this envelope of mean change [Jones, 2010a]. The shift was rapid, noticeably affecting water resources, ecosystems, heat-related risks and agriculture [Chessman, 2009; Jones, 2009, 2010a, 2010b; Mac Nally *et al.*, 2009a, 2009b]. It has been compared with a similar change in southwestern Western Australia in the early 1970s [Hope *et al.*, 2010]. Rainfall reductions in both regions have been linked into increasing mean sea level pressure over southern Australia [Hope *et al.*, 2010]. Analyzing the role of natural variability and anthropogenic influences will help determine whether this change is temporary or part of a long-term process. Existing techniques for detecting nonlinear changes in time series of climate variables [Vives and Jones, 2005], analyzing regional climate relationships [Karoly and Braganza, 2005b; Nicholls, 2003; Nicholls *et al.*, 2004; Power *et al.*, 1998] and pattern scaling [Mitchell, 2003; Whetton *et al.*, 2005], were combined to assess observed changes. The method was repeated with climate model output to determine whether the models display similar dynamics. Methods for incorporating nonlinear changes in the analysis and communication of regional climate change are discussed.

2. The Region

[7] The study region is southeastern Australia south of 33°S and east of 135°E, covering mainland SEA and Tasmania. Annual average rainfall of about 625 mm peaks in winter-spring, average daily temperature is 14.6°C with an average maximum of 20.6°C and average minimum of 8.6°C (1910–2010). Attribution studies have linked the post-1996 warming to anthropogenic regional warming and broader teleconnections affecting regional rainfall [Hope *et al.*, 2010; Kearney *et al.*, 2010; Murphy and Timbal, 2008; Nicholls, 2010; Timbal *et al.*, 2010].

[8] For rainfall, the South-Eastern Australian Climate Initiative (SEACI) Stage 2 project covering the SEA mainland south of 33.5°S and east of 135.5°E concluded that:

[9] 1. The strengthening of the sub-tropical ridge (STR) during 1997–2008 accounts for up to 80% of the observed rainfall decline in the southwestern part of Eastern Australia.

[10] 2. Climate modeling was best able to simulate the observed decline in rainfall and the intensification of the STR over SEA if both anthropogenic and natural external forcing was applied, although the simulated intensification was less than observed.

[11] 3. There are no statistically significant long-term trends in the intensity of the STR in the simulations with natural forcing alone [Timbal *et al.*, 2010].

[12] Therefore, studies of both regional temperature and rainfall have attributed an anthropogenic influence to recent changes.

3. Data and Method

3.1. Data

[13] Historical climate was analyzed using data from the BoM Australian rainfall and surface temperature portal [Jones *et al.*, 2004] averaged for SEA from all Australian rainfall data [Jones *et al.*, 2009] and high-quality temperature data [Della-Marta *et al.*, 2004]. The rainfall data were interpolated from individual station records onto a 0.05° grid and temperature from homogenized station data onto a 0.25° grid from individual stations [Jones *et al.*, 2009]. Time series (1910–2010) of regional annual average daily maximum and minimum temperature (T_{max} , T_{min}) and monthly precipitation total (P) for SEA south of 33°S and east of 135°E were extracted. Climate model output of the same variables from the eleven climate models having such data available, was extracted from the World Climate Research Programme's (WCRP's) Coupled Model Intercomparison Project phase 3 (CMIP3) multimodel data set and annual averages for the study region were calculated (Table 1). Zonal and hemispheric average annual temperature anomaly data (T_{av}) from the zonal, hemispheric and global temperatures from the Goddard Institute of Space Studies (GISS) data sets [Hansen *et al.*, 1999, 2001], comprising the GHCN-V2 land temperature and HADISST1/Reynolds v2 sea surface temperature, contributed to a wider-scale analysis of observed temperature. Globally averaged temperature anomalies from the Hadley Centre – Climate Research Unit HadCRUt3 [Brohan *et al.*, 2006] were also used. Both sets of anomalies were from a baseline of 1961–1990.

3.2. Method

[14] The process involves the following steps: (1) identification of a stationary climate period using step changes in paired annual data; (2) calculation of regression relationships between co-varying climate variables for that period; (3) identification of externally driven warming using the residuals of those relationships analyzed for the non-stationary period; this assumes that the relationships between co-varying variables as influenced by natural climate variability remain constant over time; and (4) analysis of nonlinear behavior in observed and modeled regional climate.

[15] The core analytic technique is the detection of multiple shifts in climate variables, sometimes combined with trending behavior. This is carried out using the bivariate test of Maronna and Yohai [1978], which assumes a serially independent sequence $\{x_i, y_i\}$ of n two-dimensional random vectors, each distributed normally. The mean of $\{y_i\}$ is tested against $\{x_i\}$, using a likelihood ratio test producing

Table 1. The Global Climate Models Used for Simulations of 20th and 21st Century Climate in SEA^a

Modeling Group	Model Name	Run Number	Horizontal Resolution (km)	Emission Scenario	Forcings	Warming (°C)	M Skill Score
CSIRO, Australia	CSIRO-MK3.0	1	~175	A1B	G, O, SD	2.28	0.601
		1	~175	A2	G, O, SD	3.08	0.601
CSIRO, Australia	CSIRO-MK3.5	1	~175	A1B	G, O, SD	3.83	0.607
		1	~175	A2	G, O, SD	4.47	0.607
NASA/Goddard Institute for Space Studies, USA	GISS-AOM	1	~300	A1B	G, SD, SS	2.56	0.564
		2	~300	A1B	G, SD, SS	2.55	0.564
Centre for Climate Research, Japan	MIROC-MR	2	~250	A1B	G, O, SD, BC, OC, MD, SS, LU, SO, V	3.74	0.608
		2	~250	A2	G, O, SD, BC, OC, MD, SS, LU, SO, V	4.14	0.608
		3	~250	A1B	G, O, SD, BC, OC, MD, SS, LU, SO, V	3.61	0.608
		3	~250	A2	G, O, SD, BC, OC, MD, SS, LU, SO, V	4.09	0.608
National Center for Atmospheric Research, USA	NCAR-CCSM	9	~125	A1B	G, O, SD, BC, OC, SO, U	3.29	0.677

^aThe forcing factors are: G, greenhouse gases; O, ozone; SD, sulfate direct; BC black carbon; OC, organic carbon; MD, mineral dust; SS, sea salt; LU, land use; SO, solar irradiance; V, volcanic aerosol. Also given is global mean warming 2091–2100 from the pre-1900 mean. The M skill score is for the Australian region [CSIRO and BoM, 2007].

the test statistic T_i , measuring a step change in an otherwise stationary series. Each of $\{x_i, y_i\}$ are standardized for all of j before computing the test statistics:

$$\text{Let } X_i = \frac{1}{i} \sum_{j=1}^i x_j \text{ and } Y_i = \frac{1}{i} \sum_{j=1}^i y_j \quad \text{for all } i < n$$

$$S_{xy} = \sum_{j=1}^n x_j y_j$$

$$F_i = n - \frac{[X_i^2 ni]}{(n - i)} \quad \text{for all } i < n$$

$$D_i = \frac{(S_{xy} X_i - n Y_i) n}{(n - i) F_i} \quad \text{for all } i < n$$

$$T_i = \frac{i(n-i) D_i^2 F_i}{(n^2 - S_{xy}^2)} \quad \text{for all } i < n$$

$$T_{i0} = \max_{i < n} [T_i] \text{ and } i_0 \text{ is the value of } i \text{ for which } T_i \text{ is a maximum}$$

[16] If $p(T_{i0})$ is above a given statistical threshold, then a step change can be said to have occurred in the following year with a given confidence. Significance for $n = 10$ to 70 are provided by Maronna and Yohai [1978] and $n = 100$ by Potter [1981].

[17] In climatology, this test has been used to detect inhomogeneities in time series of climate variables [Bücher and Dessens, 1991; Potter, 1981], and also to measure changes in streamflow relative to P and Tav and P to Tav in the USA [Lettenmaier *et al.*, 1994] and P relative to T_{max} in Northern America [Gan, 1995]. Where such shifts occur across a region, and artificial inhomogeneities and immediate local effects can be ruled out, the principle of regional homogeneity suggests that a shift in climate regime has occurred. Methods used for testing regime shifts were assessed by Rodionov [2005]. He did not include the bivariate test but reviewed the standard normal homogeneity test of Alexandersson [1986] which performs similarly – it works well with shifts that are not adjacent but is weak at

the beginning and end of time series [Easterling and Peterson, 1995; Rodionov, 2005]. The bivariate test is used here because of its earlier success in identifying regime shifts in Australian rainfall and temperature [Jones, 2010b; Vivès and Jones, 2005]. It is sensitive to auto-correlation, so for observed and simulated time series before the year 2000, tests were repeated where time series before and after a shift were randomized using bootstrapping. If the data are not sufficiently independent a shift will no longer register as statistically significant. The STARS test [Rodionov, 2006], which uses the t-test with pre-whitening to remove auto-correlation effects, and algorithms that improve its performance near the ends of time series, was used as a back-up test to check the robustness of the results for single variables.

[18] Three types of change may register as statistically significant in the bivariate test: (1) an abrupt change in a serially independent variable, (2) an acceleration or deceleration in a trend that is serially dependent and (3) a very large ($>2-3\sigma$) temporary departure in a time series [Vivès and Jones, 2005]. A process was developed to distinguish between these effects and to analyze multiple shifts in a time series.

[19] Each target time series was initially assessed with the bivariate test using a shortened window run at successive annual steps: a 40-year window for single variables against a randomized reference time series and an 80-year window for co-dependent variables. Strong step changes will register as single years when $T_{i0} p H_0 < 0.05$ occurs repeatedly. A gradual trend will not register as significant, but a strong accelerating trend without a shift will produce $p(T_{i0}) < 0.05$ over successive years, rather than as a step. This allows step changes and accelerating trends to be differentiated. Years with $p(T_{i0}) < 0.05$ occurring at least five times were used to segment each time series. All segments of maximum length containing one $T_{i0} \times 5$ value were then identified. These segments were re-tested using the bivariate test and results $p H_0 < 0.01$ retained. Single variables were tested against a stationary reference time series of random numbers for 100 iterations after Vivès and Jones [2005]. Co-dependent variables could be tested just the once due to a static reference.

[20] Effects of autocorrelation and temporary departures in 19th and 20th century observed and simulated records were checked by bootstrapping time series before and after shift dates to confirm statistical significance, thus ensuring that the stationary period was identified appropriately. Step changes for single variables in complete time series were also checked using Rodionov's [2006] STARS method. Settings for the latter method were determined by using observed, model simulated and artificially generated data (a trend with a super-imposed random walk of $n = 2$ and $n = 7$ years and step changes spaced at least 15 years apart). This also ensured that both statistical tests could reproduce the same shifts in artificial data, which they did to within one year. The relationships between T_{max} and P , and T_{max} and T_{min} (see Table 2 for symbol derivation) could not be tested using Rodionov's method because it does not use a reference time series.

[21] The detection phase identified the transition from stationarity to non-stationarity by identifying step changes in the relationships between the co-dependent climate variables, T_{max} and P , and T_{max} and T_{min} . These pairs are inversely correlated and correlated, respectively, for Australia on timescales from days to years [Coughlan, 1979; Nicholls, 2003; Nicholls et al., 2004]. They have a linear relationship. Power et al. [1998] found significant correlations between annual average T_{max} and total P across most of Australia, weaker in some coastal areas and absent on offshore islands. The relationship between T_{max} and P changed during the early 1970s when T_{max} increased relative to P , and coincides with a simultaneous change in the Southern Oscillation Index (SOI) [Power et al., 1998; Nicholls, 2003]. By removing co-dependency between T_{max} and T_{min} , Power et al. [1998] linked the residuals of the $T_{\text{min}}\text{-}T_{\text{max}}$ relationship to higher rainfall totals. A climate simulation forced by observed sea surface temperatures cohesively linked T_{max} and P over most areas from 40°N–40°S except for North Africa [Power et al., 1998]. Globally, negative correlations between temperature and rainfall dominate over land [Trenberth and Shea, 2005] but some locations vary on a seasonal basis, and correlations may be positive in high latitudes [Madden and Williams, 1978; Trenberth and Shea, 2005]. Douville [2006] removed the P signal from T_{av} over Sudan and Sahel to clarify the warming signal in eleven climate simulations. Karoly and Braganza [2005b] found good agreement between models and observations for T_{max}/P and $T_{\text{max}}/T_{\text{min}}$ over Australia, southern Australia and SEA, concluding that observed changes in T_{max} and T_{min} were very likely to be of anthropogenic origin.

[22] The working hypothesis is that during episodes of natural variability, temperature and rainfall are quasi-stationary, subject to changes in phenomena such as ENSO [Nicholls et al., 2004; Power et al., 1998]. Relationships between T_{max}/P and $T_{\text{max}}/T_{\text{min}}$ are linear; a step change in natural variability will see correlated variables change together. Externally forced step changes will introduce non-stationary behavior between correlated variables as observed by Nicholls [2003] for recent warming in Australia. Inter-annual variability was lower for some model-generated variables than for observations; e.g., simulated σT_{min} averaged 0.3°C compared to 0.5°C for observations. Climate was therefore considered to be non-stationary if a step change

of at least 1σ in T_{max}/P or $T_{\text{min}}/T_{\text{max}}$ occurred, a stricter criterion than a threshold of $pH_0 = 0.01$.

[23] Regressions producing T_{max}_P , $T_{\text{max}}_{T_{\text{min}}}$ and $T_{\text{min}}*_P$ were conducted using T_{max} , T_{min} and P for the stationary period in the observations and each of the models where:

$$y = \alpha + \beta x \quad (1)$$

[24] The residuals of those relationships is

$$e = y - \hat{y} \quad (2)$$

where \hat{y} is the predictand, are then estimated and assumed to be independent of x and y .

[25] T_{max}_P and $T_{\text{max}}_{\text{ARW}}$ (Anthropogenic Regional Warming: ARW) represent the influence of P and anthropogenic global warming (AGW), respectively, in the non-stationary period (equations (2) and (3)). T_{max}_P will include a measure of change due to any anthropogenic influences on P , but P has to be estimated independently to gauge that effect.

$$T_{\text{max}}_P = \alpha + \beta P \quad (3)$$

$$T_{\text{max}}_{\text{ARW}} = T_{\text{max}} - T_{\text{max}}_P \quad (4)$$

$T_{\text{min}}_{T_{\text{max}}}$ represents the influence of T_{max} on T_{min} , $T_{\text{min}}*_P$ accounts for rainfall effects (generally small). Also added is the indirect effect of increasing $T_{\text{max}}_{\text{ARW}}$ on T_{min} . $T_{\text{min}}_{\text{ARW}}$ accounts for the influence of AGW on regional T_{min} .

$$T_{\text{min}}_{T_{\text{max}}} = \alpha + \beta T_{\text{max}} \quad (5)$$

$$*P = T_{\text{min}} - T_{\text{min}}_{T_{\text{max}}} \quad (6)$$

$$T_{\text{min}}*_P = \alpha + \beta *P \quad (7)$$

$$T_{\text{min}}_{\text{ARW}} = T_{\text{min}} - T_{\text{min}}_{T_{\text{max}}} + T_{\text{min}}*_P + \beta T_{\text{max}}_{\text{ARW}} \quad (8)$$

The β factor in equation (8) is taken from equation (5).

[26] $T_{\text{max}}_{\text{ARW}}$ and $T_{\text{min}}_{\text{ARW}}$ were then analyzed with the bivariate test to assess shifts in the anthropogenic signal. $T_{\text{max}}_{\text{ARW}}$ and $T_{\text{min}}_{\text{ARW}}$ were then regressed against mean anthropogenic global warming (AGW) for the entire historical period following the method for pattern scaling described by Whetton et al. [2005]. AGW was measured as an anomaly from a baseline of 1910 for the historical data and pre-1900 for the model data. Regressions of model data were repeated for the historical period of non-stationarity.

4. Results

4.1. Observed Climate

[27] Bivariate analysis of the historical data reveals statistically significant step changes for T_{max} , T_{min} , T_{max}/P and $T_{\text{min}}/T_{\text{max}}$ (Table 3). The sustained regional deficit in rainfall over the months of March–October began in October 1996 [Bureau of Meteorology, 2006]. A very wet year in 2010 caused by a combined La Niña–negative Indian Ocean Dipole event removed any statistical significance from the regional average deficit, which for 1910–2009 measured −102.5 mm in 2001 at $pH_0 = 0.05$. Of the individual

Table 2. Symbols Used

Symbol	Measure	Unit
T_{av}	Average annual air temperature	°C
T_{max}	Maximum annual air temperature	°C
T_{min}	Minimum annual air temperature	°C
P	Precipitation	mm
DTR	Diurnal temperature range	°C
T_{max}/P	T_{max} tested using P as a reference	°C
T_{min}/T_{max}	T_{min} tested using T_{max} as a reference	°C
$T_{max,P}$	T_{max} calculated from a linear regression with P	°C
$T_{min,T_{max}}$	T_{min} calculated from a linear regression with T_{max}	°C
δT_{max}	Change in T_{max}	°C
δT_{av}	Change in T_{av}	°C
δT_{min}	Change in T_{min}	°C
δP	Change in P	mm
δDTR	Change in diurnal temperature range	°C
$*P$	Residual of $T_{min,T_{max}} - T_{min}$; P factor in T_{min}	°C
$T_{min}*_P$	$T_{min,T_{max}}$ summed with its residual regressed against P	°C
$T_{max,ARW}$	Anthropogenic component of regional T_{max}	°C
$T_{min,ARW}$	Anthropogenic component of regional T_{min}	°C
AGW	Anthropogenic global warming	
ARW	Anthropogenic regional warming	
°C _{AGW}	Change per degree AGW	
α	Constant in linear regression	
β	Slope in linear regression	
σ	Standard deviation	
T_i	Test statistic for the bivariate test	
T_{i0}	Maximum test statistic for the bivariate test	
$p(T_{i0})$	Probability of test statistic	

seasons, only autumn (March–May) shows a shift of any significance: -40.9 mm in 1991 at $p H_0 = 0.05$. A number of influences affect regional rainfall [Nicholls, 2010; Timbal, 2009; Ummenhofer *et al.*, 2009], suggesting that the recent deficit is unlikely to have a single cause. These changes also vary across the region; e.g., in southern SEA individual homogenized precipitation and streamflow time series to 2009 show an annual shift of $p H_0 = 0.01$ in 1997 [Jones, 2009]; further north 2002 becomes a more prominent shift date.

[28] T_{max} undergoes a significant upward shift of 0.8°C from 1997 and T_{min} shifts upward by 0.7°C from 1973

(Table 3). Both variables shift with respect to their close correlates, P and T_{max} , in 1999 and 1968. Nicholls [2003] found that the relationship between P , T_{max} and T_{min} in New South Wales changed from 1973 onwards. The period of stationarity was therefore selected as 1910–1967 and non-stationarity 1968–2010.

[29] The results are shown in Figure 1. In the first half of the record, T_{max} , $T_{max,P}$ and $T_{max,ARW}$ vary closely with each other but after 1970, most of the warming in T_{max} is attributed to ARW. T_{min} shows the influence of increasing T_{max} from 1997. Using the bivariate test, $T_{max,ARW}$ shifts upward by 0.5°C in 1973 at $p < 0.01$ and by 0.4°C in 1999 at $p = 0.05$ and $T_{min,ARW}$ shifts upward by 0.7°C in 1968 with little trend afterwards (0.05°C per century). Figure 2 shows statistically significant step changes for T_{max} , T_{min} , $T_{max,ARW}$ shifts and $T_{min,ARW}$ shifts with intervening trends. T_{max} shows a statistically significant shift in 1997 but $T_{max,ARW}$ shows an underlying shift of 0.4°C in 1973 that was masked by temporarily increased P . T_{min} shifts upward in 1973 and is followed by a non-significant positive trend, but when the influence of T_{max} and P are removed, the shift occurs in 1968 with no trend before and a non-significant trend after.

[30] When step changes and trends combine in a time series, measurement of each component becomes difficult [McDowall *et al.*, 1980]. Here, three methods of measuring change are compared: (1) simple trend analysis; (2) separation of temperature time series into segments separated by statistically significant step changes and differencing the means; and (3) as for item 2 with separate measurement of significant trends within segments. The preference of one method over another will depend on its utility for decision-making. Simple trend analysis (method 1) for 1910–2010 shows an increase in T_{max} of $0.68 \pm 0.05^\circ\text{C}$, in T_{min} of $1.11 \pm 0.04^\circ\text{C}$ and in T_{av} of $0.89 \pm 0.04^\circ\text{C}$. The estimated influence of ARW on T_{av} using this method is $0.77 \pm 0.05^\circ\text{C}$ (Table 4).

[31] For method 2, the T_{max} -related time series (T_{max} , $T_{max,P}$ and $T_{max,ARW}$) were separated into the segments 1910–1972, 1973–1996 and 1997–2010 based on step changes within those records. The T_{min} - (T_{min} , $T_{min,T_{max}}$, $T_{min}*_P$ and $T_{min,ARW}$) and T_{av} -related time series were separated into 1910–1967, 1968–1996 and 1997–2010 segments. The differences between means total $0.87 \pm 0.09^\circ\text{C}$ for T_{max} , $0.92 \pm 0.10^\circ\text{C}$ for T_{min} and $0.89 \pm 0.09^\circ\text{C}$ for T_{av} . This is a more appropriate measure of change than

Table 3. Historical Data for Southeastern Australia With Results of Bivariate Test Showing the Statistic at the Year of Change (T_{i0}), the Year of Change ($T_{i0} + 1$), the Size of the Change and Significance, and the STARS Test Set at $p H_0 < 0.05$ Showing the Year and Size of Change

	Average	Standard Deviation	Bivariate				STARS	
			T_{i0}	Year	Change	Significance	Year	Change
P (mm)	628.6	107.9	3.8	2010	154.6	None	2010	None
T_{max} (°C)	20.6	0.6	24.3	1997	0.8	<0.01	1997	0.8
T_{min} (°C)	8.6	0.5	45.8	1973	0.7	<0.01	1968	0.6
							2007	0.7
T_{av} (°C)	14.6	0.5	36.8	1972	0.6	<0.01	1972	0.7
	14.9	0.4	12.9	1999	0.5	0.01	1999	0.5
T_{max}/P (°C)	20.6	0.6	21.2	1999	0.7	<0.01		
T_{min}/T_{max} (°C)	8.6	0.5	36.6	1968	0.6	<0.01		

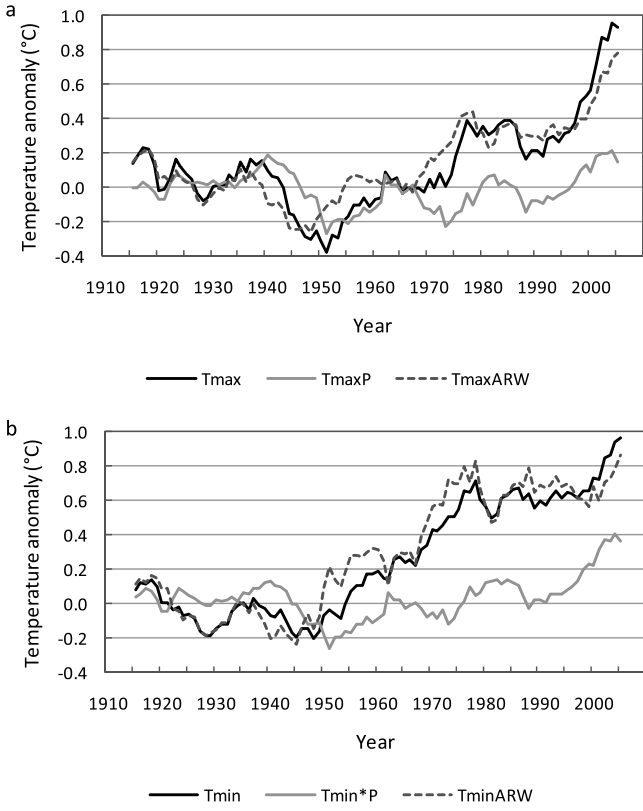


Figure 1. Anomalies for (a) T_{max} , T_{max}^P and T_{max}^{ARW} , and (b) T_{min} , T_{min}^P and T_{min}^{ARW} . Anomalies are measured from a baseline period of 1910–1967 and are shown as an 11-year running mean.

Table 4. Changes in Observed and Derived Variables for South-eastern Australia 1910–2010 Using Three Methods: Linear Trend, Step Changes (Differences of Means) and Step Changes With Significant Trends^a

Variable	Linear Trend	Step Changes	Step + Trend
T_{max}	0.68	0.87	1.08
T_{max}^P	0.03	0.16	0.08
T_{max}^{ARW}	0.65	0.71	1.00
T_{min}	1.11	0.92	1.16
T_{min}^P	0.21	0.26	0.33
T_{min}^{ARW}	1.08	0.79	1.10
T_{av}	0.89	0.89	1.12
T_{av}^{ARW}	0.87	0.75	1.05
<i>Anthropogenic Component</i>			
T_{max}	96%	82%	93%
T_{min}	98%	86%	95%
<i>Total</i>	97%	84%	94%

^aAlso shown is the estimated anthropogenic component for each method.

method 1 because there is no attributable warming prior to 1967: a linear trend from 1910 will over-estimate earlier warming and under-estimate later warming.

[32] Method 3 differences the means as in method 2 and factors in a warming trend from 1997, triggered by a statistically significant trend (0.46°C per decade at $pH_0 < 0.05$) in T_{max}^{ARW} from 1997 to 2010. T_{max} increases by $1.08 \pm 0.09^{\circ}\text{C}$, T_{min} by $1.16 \pm 0.10^{\circ}\text{C}$ and T_{av} by $1.12 \pm 0.09^{\circ}\text{C}$. These changes are largest because they factor in a rising trend from 1997. The decision-making context of this method is informed by this upward trending warming that may well continue. The evolution of warming during the late 20th century where step changes with minimal intervening trends grade into step changes with increasing trends is

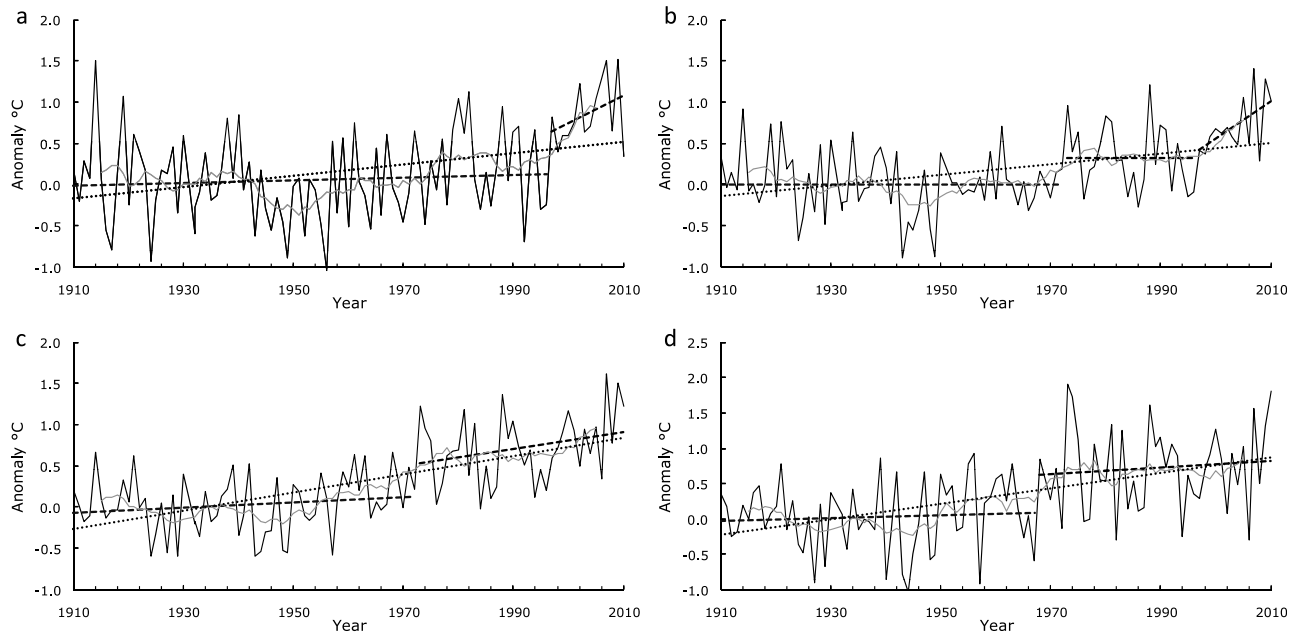


Figure 2. Observed annual (a) T_{max} , (b) T_{max}^{ARW} , (c) T_{min} and (d) T_{min}^{ARW} (black line) anomalies for SEA 1910–2010 with five-year running mean (thin gray line), linear trend (dotted line) and linear trends separated by statistically significant step changes (dashed lines).

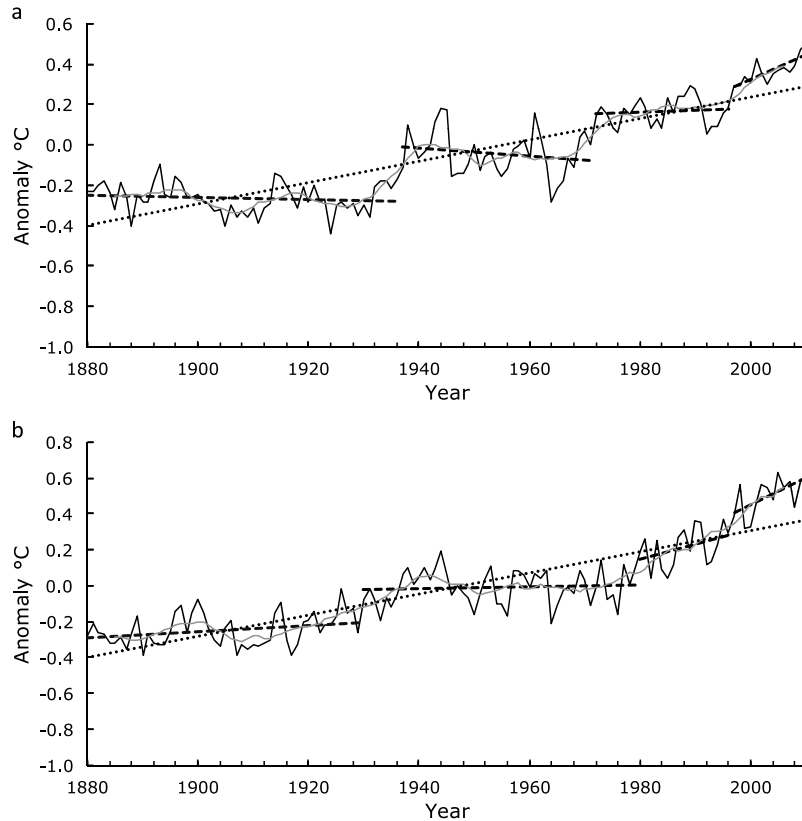


Figure 3. Observed annual T_{av} for (a) GISS 24–44°S and (b) GISS global mean 1880–2010 anomalies (1961–90) with five-year running mean (thin gray line), linear trend (dotted line) and linear trends separated by statistically significant step changes (dashed lines).

typical of regional simulations for SEA, as will be shown in the next section.

[33] The anthropogenic component attributed to δT_{av} is 97% and 94% for Methods 1 and 3 and 84% for method 2. This suggests that the majority of observed regional warming is anthropogenic and that most of that warming has occurred since 1968. The year 1968 coincides with a statistically significant step change in the density of low pressure systems in southern Australia (1950–1998) of 0.9 at $P < 0.01$ within a long-term average of 7.4 per $^{\circ}\text{lat}^2$ (1950–2008). The same year also marks a downward shift in mean rainfall [Vivès and Jones, 2005] and frequency of daily falls over 30 mm [Li *et al.*, 2005] in southwest Western Australia. Changes in growth rates of storm tracks affecting southern Australia from a baseline of period 1946–67, are a 34% decrease in 1975–1994 and a further 37% decrease in 1997–2006 [Fredriksen *et al.*, 2010].

[34] The changes in SEA were compared with step changes in global temperatures from the HadCRU data set [Brohan *et al.*, 2006] and zonal, hemispheric and global temperatures from the GISS data sets [Hansen *et al.*, 1999, 2001]. The GISS zonal average for T_{av} 1880–2010 covering 24–44°S shows step changes ($pH_0 < 0.01$) of 0.22°C in 1937, 0.21°C in 1972 and 0.20°C in 1997 (Figure 3a). Southern hemisphere T_{av} shows step changes of similar magnitude in 1936, 1969 and 1996 but also shows upward trends after 1969. Globally, the HadCRU and GISS (Figure 3b) data sets show step changes in 1930–31, 1979–80 and 1997, the

latter being 0.3°C. Therefore, regional temperature shifts have zonal and hemispheric links for the first set of step changes in 1968–73 and global links for the latter step change in 1997.

[35] Annual correlations between detrended $T_{max,ARW}$ for SEA and T_{av} for 24–44°S are 0.05 from 1910 to 1945 and 0.57 from 1946 to 2010, suggesting that there was no discernible influence on regional temperature before 1946 (Figure 4). The timing of step changes covering the periods 1968–73 and 1997 are therefore shared by SEA, GISS 24–44°S and the southern hemisphere, whereas 1935–36 is absent from SEA. Up to the late 1940s temperature in SEA varied independently of regional climate but subsequently became entrained into broader warming patterns.

4.2. Simulated Climate

[36] Output for SEA from eleven model simulations was analyzed using the bivariate moving window test to identify robust shifts. Due to shared 20th century runs but different 21st century projections for some models, only six independent 20th century simulations were available. Statistically significant step changes in each model averaged about 3.5 per run for T_{max} and 4.5–5.5 per run for T_{min} . No shifts $> 1\sigma$ were identified for P , but many of the step changes were large enough to produce significant hydroclimatic and ecological impacts if experienced in the real world.

[37] Table 5 shows the periods of stationarity for observations and climate models. Non-stationarity in the climate

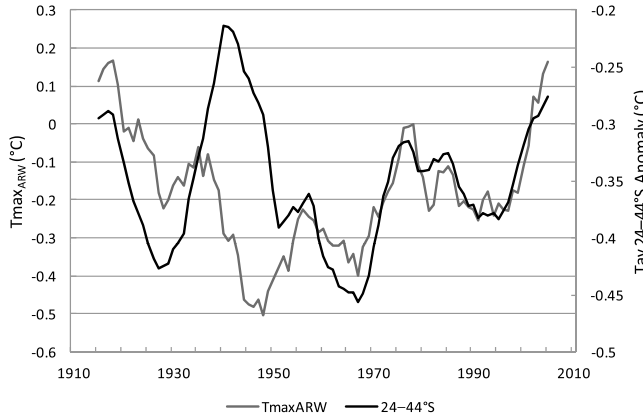


Figure 4. The 11-year running means of SEA $T_{\max,ARW}$ and GISS T_{av} anomaly ($24\text{--}44^{\circ}\text{S}$), detrended and contrasted on separate axes. Annual correlation to 1946 is 0.05, after 1946 is 0.57.

models commenced between 1963 and 2002 with the T_{\min}/T_{\max} relationship shifting first. Initial step changes in T_{\max}/P ranged from 0.6°C to 1.5°C , compared to the historical shift of 0.7°C . Step changes in T_{\max} were of a similar magnitude. Changes in T_{\min} were smaller but more frequent (Figure 5). Approximately two-thirds of shift dates were shared between the bivariate and STARS methods. A few significant shifts occurred during the periods of stationary climate, mainly in the MIROC model, but most occurred during non-stationary periods.

[38] Rainfall variability can also influence the timing and magnitude of step changes. Figure 6 shows T_{\max} , T_{\min} , $T_{\max,ARW}$ and $T_{\min,ARW}$ from the CSIRO Mk3.5 A1B and MIROC MR3 A1B simulations. In the CSIRO simulation, rainfall decreases amplify step changes in warming. T_{\max} undergoes four significant step changes of up to 1.5°C , whereas $T_{\max,ARW}$ undergoes more but smaller step changes and by 2100 warms by 0.6°C less. $T_{\min,ARW}$ also warms by slightly less than T_{\min} . In the MIROC simulation, increasing P suppresses step changes and total warming in T_{\max} and T_{\min} to 2100 by about 0.2°C .

[39] Projected warming is usually estimated by differencing future decadal periods with the baseline or by pattern scaling change per degree of global warming. Such methods smooth

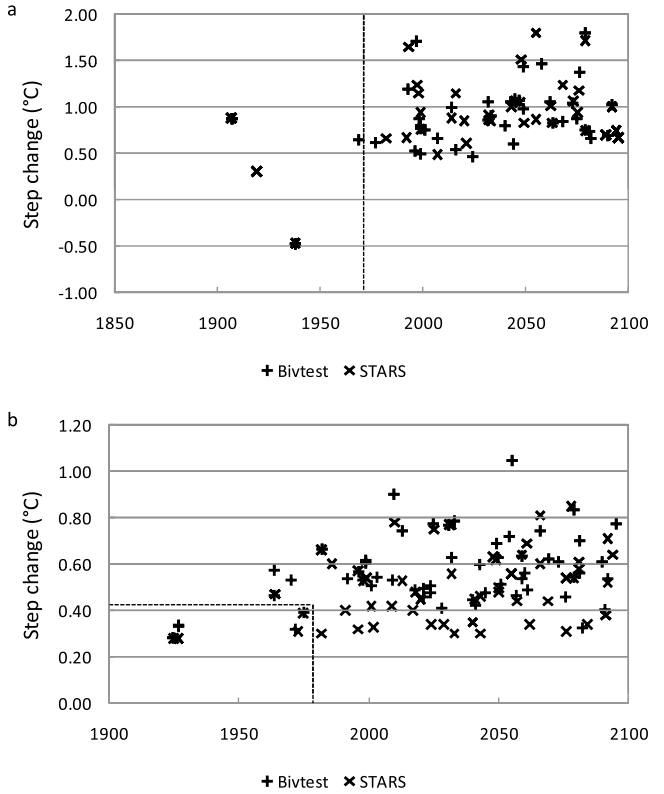


Figure 5. Statistically significant step changes using the bivariate test ($pH_0 < 0.01$) and STARS test ($pH_0 < 0.05$, 15 year samples, pre-whitened) for (a) T_{\max} and (b) T_{\min} over SEA from eleven climate models. Points to the left of the dashed line occur during stationary climate.

out any variation in the warming signal, the first by implication and the second by design. Here T_{av} , T_{\min} , T_{\max} , $T_{\max,ARW}$, $T_{\min,T_{\max}}$ and $T_{\min,ARW}$ were scaled per degree of global warming ($^{\circ}\text{C}_{\text{AGW}}$) by regressing each against the mean global temperature anomaly with respect to the pre-1900 average, following the method of Whetton *et al.* [2005]. Observations were analyzed using HadCRU and GISS global mean warming data and averaged. Scaling was carried out for the entire record and for 1968–2010, the period of non-stationarity in the observations. The results

Table 5. Data Source and Year of First Change Greater Than One Standard Deviation From the Data Measured for T_{\max} Against P and T_{\min} Against T_{\max} Using the Bivariate Test^a

Model	T_{\max}/P			T_{\min}/T_{\max}			Stationary Period (SEA)
	T_{i_0}	Year	Change	T_{i_0}	Year	Change	
Observations	21.2	1999	0.7	36.6	1968	0.6	1910–1967
CSIRO Mk3 A1B	124.4	2047	1.8	85.5	1992	0.6	1871–1991
CSIRO Mk3 A2	63.3	2006	0.9	92.1	1998	0.7	1871–1991
CSIRO Mk3.5 A1B	55.2	1996	1.1	16.4	1964	0.4	1871–1963
CSIRO Mk3.5 A2	57.0	1996	1.1	32.7	1964	0.4	1871–1963
GISS AOM R1 A1B	150.6	2000	1.5	34.0	1983	0.4	1850–1982
GISS AOM R2 A1B	49.7	1982	0.6	61.3	1982	0.6	1850–1981
MIROC Medres R2 A1B	55.1	1999	0.8	39.0	1999	0.5	1850–1998
MIROC Medres R2 A2	70.9	1999	0.9	47.5	1999	0.5	1850–1998
MIROC Medres R3 A1B	51.5	2007	0.7	27.9	2003	0.5	1850–2002
MIROC Medres R3 A2	68.9	2016	1.0	21.6	2001	0.5	1850–2000
NCAR CCSM3 A1B	47.2	1986	0.8	38.9	1971	0.5	1870–1970

^aThe resulting stationary period for analysis is also shown.

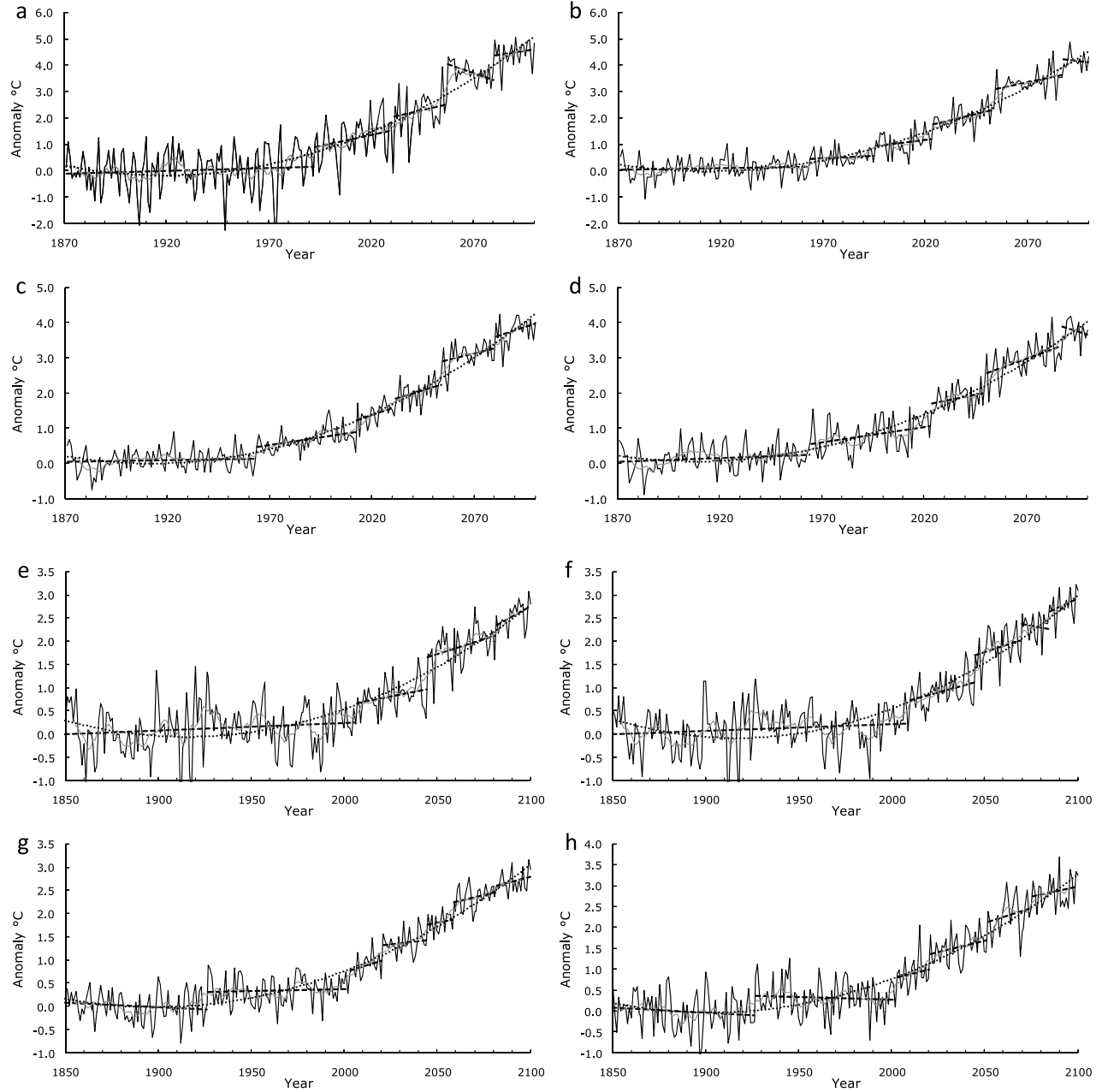


Figure 6. Annual (a) T_{max} , (b) $T_{\text{max,ARW}}$, (c) T_{min} and (d) $T_{\text{min,ARW}}$ (black line) anomalies for SEA 1871–2100 from the CSIRO Mark3.5 A1B simulation. Annual (e) T_{max} , (f) $T_{\text{max,ARW}}$, (g) T_{min} and (h) $T_{\text{min,ARW}}$ (black line) for SEA 1850–2100 from the MIROC MR3 A1B simulation. All charts include five-year running mean (thin gray line), quadratic trend (dotted line) and linear trends separated by statistically significant step changes (dashed lines).

contrast the standard method of assessing T_{av} as a function of average global warming with T_{max} and T_{min} partitioned according to internal and external climate forcing.

[40] Average δT_{av} from the climate models is $0.93^{\circ}\text{C}_{\text{AGW}}$ to 2100 and $0.98^{\circ}\text{C}_{\text{AGW}}$ over 1968–2010, similar to observations for the same period (Table 6). $T_{\text{max,ARW}}$ over 1968–2010 from models is $0.87^{\circ}\text{C}_{\text{AGW}}$ compared to $0.88^{\circ}\text{C}_{\text{AGW}}$ for observations. However, average $T_{\text{min,ARW}}$ over 1968–2010 of $0.84^{\circ}\text{C}_{\text{AGW}}$ in the models is lower than the observed trend of $1.27^{\circ}\text{C}_{\text{AGW}}$. The timing of abrupt changes clearly affects trend analysis. The observed trend

for $T_{\text{min}}^{\circ}\text{C}_{\text{AGW}}$ is $0.26^{\circ}\text{C}_{\text{AGW}}$ higher than $T_{\text{max}}^{\circ}\text{C}_{\text{AGW}}$ despite there being only 0.05°C difference in mean change, because the earlier 1968 shift in T_{min} occurred during a period of lower global warming.

[41] The timing of step changes also influences the spread of pattern-scaled trends over 1968–2010. If internal climate variability is driving the step changes then removing its effects would reduce the standard deviation of the model sample, but over 1968–2010 it reduces from 0.31 to 0.25 for T_{max} and $T_{\text{max,ARW}}$ and increases from 0.12 to 0.15 for T_{min} and $T_{\text{min,ARW}}$. The timing of step changes among

Table 6. Change per Degree of Global Warming for Observed and Simulated Climate Variables for 1910–2010 (Observations), Pre-industrial to 2100 Simulations From 11 Climate Models and 1968–2010 for Observations and Models Over SEA

Model	Tav	Tav 68–10	Tmax	Tmax _{ARW}	Tmax 68–10	Tmax _{ARW} 68–10	Tmin	Tmin _{Tmax}	Tmin _{ARW}	Tmin 68–10	Tmin _{ARW} 68–10
Observations	0.93	1.10	0.80	0.71	0.93	0.87	1.06	0.30	1.04	1.27	1.27
CSIRO Mk3 A1B	1.05	1.30	1.15	1.10	1.40	1.31	0.95	0.23	0.94	1.20	1.17
CSIRO Mk3 A2	0.96	1.06	1.03	0.97	1.19	1.08	0.89	0.21	0.87	0.93	0.90
CSIRO Mk3.5 A1B	1.06	0.86	1.14	1.03	0.87	0.84	0.98	0.27	0.94	0.85	0.84
CSIRO Mk3.5 A2	1.06	0.94	1.13	1.02	0.98	0.87	0.98	0.27	0.93	0.90	0.86
GISS AOM R1 A1B	0.90	0.89	0.88	0.82	0.77	0.80	0.92	0.44	0.88	1.00	1.03
GISS AOM R2 A1B	0.89	0.88	0.90	0.80	0.88	0.71	0.89	0.47	0.82	0.87	0.76
MIROC MR R2 A1B	0.86	1.19	0.92	0.86	1.47	1.08	0.80	0.33	0.77	0.91	0.63
MIROC MR R2 A2	0.88	1.25	0.91	0.89	1.48	1.12	0.86	0.31	0.84	1.03	0.77
MIROC MR R3 A1B	0.78	0.76	0.71	0.75	0.60	0.47	0.85	0.23	0.88	0.91	0.78
MIROC MR R3 A2	0.88	0.91	0.87	0.88	0.79	0.63	0.90	0.29	0.91	1.04	0.87
NCAR CCSM3	0.94	0.79	0.94	0.97	0.82	0.73	0.94	0.40	0.97	0.77	0.68
Model Average	0.93	0.98	0.96	0.92	1.02	0.88	0.91	0.31	0.89	0.95	0.84
Stand Dev.	0.09	0.19	0.14	0.11	0.31	0.25	0.06	0.09	0.06	0.12	0.15

the models affects the measurement of trends in a similar way to observations, which has implications for the detection and attribution of episodic change.

4.3. Testing Tmax/P and Tmax/Tmin

[42] The robustness of the assumptions used to estimate $T_{\text{max,ARW}}$ and $T_{\text{min,ARW}}$ was tested in the observational data; in particular, the stability of the co-dependent relationships between T_{max} and P and between T_{min} and T_{max} , and the criteria used to set stationarity. The relationships between co-dependent variables as described in equations (3) and (5) were analyzed for 20-year time slices overlapping every five years. This provided 11 time slices for the stationary period and 19 overall.

[43] The strength of the relationship between T_{max} and P is correlated with the standard deviation of T_{max} (σT_{max}) [see also Trenberth and Shea, 2005]. The r^2 relationship between σT_{max} during the stationary period ranged between from 0.06 to 0.75 and was stronger in warmer decades. In the non-stationary period, the α variable (constant) increased relative to σT_{max} while the β variable (slope) remained unchanged. External warming ($T_{\text{max,ARW}}$), therefore, had no detectable influence on the relationship between T_{max} and P . Short-term regressions between T_{max} and P calculated for periods ranging from 10 to 30 years, and used to estimate $T_{\text{max,ARW}}$, showed that different sampling periods had little effect. This relationship was strong early in the 20th century, weak mid-century and is currently strong.

[44] The strength of the relationship between T_{min} and T_{max} is moderated by the standard deviation of the diurnal temperature range (σDTR). The r^2 relationship during the stationary period ranged between from 0.0 to 0.50 varying inversely with σDTR , therefore is strongest when DTR is low. Again, there was no evidence of the slope of the regression changing during the non-stationary period or of sensitivity to sampling length. The results are not improved by finer temporal sampling so the use of the entire period of stationary climate to establish relationships between T_{max} and P , and T_{min} and T_{max} is robust. This is consistent with the findings of Madden and Williams [1978].

[45] The sensitivity of the results to assumptions of stationarity was also tested via a graphical interface that varied

the length of the stationary periods linked to charts of $T_{\text{max,ARW}}$ and $T_{\text{min,ARW}}$. Two sets of model simulations, the MIROC2 and MIROC3 A1B and A2 runs, showed statistically significant changes in T_{min} and T_{max} during the stationary period. When the stationary period was reset to before these changes, the resulting estimates of $T_{\text{max,ARW}}$ and $T_{\text{min,ARW}}$ remained within $\pm 0.02^\circ\text{C}_{\text{AGW}}$. These step changes are therefore interpreted as being due to internal climate variability and are not influenced by external forcing. Only when the baseline was extended well into the non-stationary period did the results begin to change appreciably. Combined with the ‘sliding window’ use of the bivariate test and the Rodionov STARS method, the identification of false positives is unlikely (selecting a shift when one has not occurred). A false negative (not selecting a shift) may overlook small changes but the results are also fairly insensitive to this type of error. Therefore, even though the method used here contains subjective elements, such as choice of thresholds for non-stationarity and the final selection of shift dates when they differ between tests, the results can be cross-checked in several ways.

5. Conclusions

[46] Step changes in the relationship between the co-dependent climate variables T_{max}/P and $T_{\text{max}}/T_{\text{min}}$ have been used to identify stationary and non-stationary periods of climate for SEA over the period 1910–2010. The stationary period spans 1910–1967. Non-stationary conditions were initiated in 1968. Two episodes of step-changes were identified: 1968–1973 and 1997. These episodes match step changes in T_{av} occurring in the latitudinal zone 24–44°S and in the southern hemisphere, suggesting widespread contemporaneous regional step changes in warming. The 1997 step change of 0.3°C in global mean atmospheric temperature is statistically significant ($pH_0 < 0.01$) at the global scale. Step changes for SEA of similar magnitude and timing to those in observations were identified and analyzed in eleven climate model simulations.

[47] The following process has been identified:

[48] 1. Observed and simulated 19th and early 20th century regional climate is stationary in both observations and

models. Step changes in rainfall and temperature that involve a joint response in correlated variables, signify internally forced climate variability.

[49] 2. Non-stationary warming is signaled by a significant step change in T_{min} independent of T_{max} , or together with T_{max} independent of P . Observed step changes in T_{max} and T_{min} in SEA and T_{av} in the southern hemisphere mid-latitudes are separated by periods of non-significant trend.

[50] 3. Simulated regional warming in the late 20th and early 21st century shows step changes with little trend in between, grading into step changes with steeper trends during the 21st century.

[51] The physical model behind the co-dependency of climate variables over land is straightforward. The energy balance near the surface is largely governed by the relationship between sensible and latent heat [Koster *et al.*, 2009]; comprising about 90% latent heat over the oceans and much more equal proportions over land [Budyko, 1977]. When the land environment is moisture-limited the ratio of latent to sensible heat increases with increasing moisture in a linear fashion [Granger, 1989; Koster *et al.*, 2009], producing an inverse relationship between rainfall and maximum temperature. These results are consistent with both observations and model simulations [Cai and Jones, 2005; Koster *et al.*, 2009]. The relationship between T_{min} and T_{max} is governed by the ability of the landmass to warm during the day, but its strength is governed by DTR . The strong correlation between DTR and P shows that this relationship is also linked to the energy balance over land.

[52] A simple model for the external warming of regional continental climate is to assume that warming is introduced as sensible heat, additional to the existing relationships between sensible and latent heat mediated by internal climate variability. The analysis carried out here suggests that this is the case – observed correlations between T_{max}/P as a function of σT_{max} and between $T_{\text{max}}/T_{\text{min}}$ as a function of σDTR remain constant during the non-stationary period to 2010. Co-dependent relationships under natural variability have continued unchanged under external forcing. This may continue to be the case unless the land surface itself changes, altering the partitioning of sensible and latent heat.

[53] The key finding is that the anthropogenic warming temperature signal for SEA expressed as $T_{\text{max,ARW}}$ and $T_{\text{min,ARW}}$ is introduced in discrete shifts. These events coincide with similar shifts in T_{av} on a hemispheric (1968–73) and global (1997–8) timescale. Other regions show shifts in T_{av} with different timing, suggesting that step changes of the type analyzed here are widespread. The impact of large scale variability interacting with global temperature was investigated by Swanson *et al.* [2009] and Swanson and Tsonis [2009] who found that instability in several modes of variability contributed to shifts in mean global warming. Swanson *et al.* [2009] interpreted the global result as variability on a monotonic warming curve, but the evidence here suggests that anthropogenic regional warming is episodic.

[54] The likely origin of these shifts is in atmospheric-ocean interactions. Recent findings by Meehl *et al.* [2011] investigating hiatus decades where atmospheric warming is static or slightly negative, show reduced trends of heat content in the shallow ocean above 300 m and increased trends in the deep ocean indicating increased deep ocean mixing during those periods, in both observations and in

simulations of 21st century climate. They also note that the observed changes are different across the major ocean basins. Douglass and Knox [2009] reconstruct the top of the atmosphere radiation balance from ocean heat content data from 1955 to 2003 finding that it shifted from negative between 1960 and 1975 to positive between 1975 and 2000 and back to negative after 2000. They suggest a link between these periods and the changes noted by Swanson and Tsonis [2009] analyzed from northern hemisphere indices. In the northern Pacific, regime shifts in climate indices were noted in 1976, 1989 and 1998 [Overland *et al.*, 2008]. The latter two coincide with statistically significant upward step changes in temperatures from 24 to 64°N in the GISS data set. The speculation here is that step changes in warming at the regional to global scale may occur in the transition between decadal modes of climate variability, perhaps associated with major upwelling events (e.g., the 1997–1998 El Niño). The evidence for SEA suggests anthropogenic warming has occurred in discrete steps, rather than experienced as a gradual trend, and is overprinted by the effects of climate variability. The latter would also include the response to anthropogenically forced changes in rainfall. The contemporaneous changes in rainfall in both southeast and southwestern Australia, and evidence of step changes in simulated P suggests that rainfall may undergo similar changes.

[55] If warming is non linear, consisting of both step changes and trends, then the signal-to-noise model may not hold for assessing how climate changes on a multidecadal basis, although it would remain valid for assessing whether climate has changed beyond the envelope of natural variability and other types of natural forcing (e.g., solar, volcanic). Abrupt shifts in regional climate will lead to abrupt changes in climate risks. For example, recent impacts in SEA after 1996 are non-trivial and include catastrophic wildfires, record periods of heat stress and sustained water shortages. Incremental adaptation planned to manage gradual change will lead to under-adaptation if such events occur, risking maladaptation in response to unanticipated, rapid change. This suggests an urgent need for further research. For example, the mechanisms causing episodic atmospheric warming need to be investigated. The statistical methods applied in this study need to be tested seasonally to determine seasonal co-variability. Other regions also need to be investigated. Last, protocols for selecting stationary and non-stationary periods and measuring climate change involving both shifts and trends would need to be developed.

[56] **Acknowledgments.** The Centre for Australian Weather and Climate Research, the Bureau of Meteorology, Dewi Kirono and David Kent of CSIRO and Bertrand Timbal of the BoM supplied climate data, model data and results from the South-Eastern Australian Climate Initiative. The WCRP CMIP3 multimodel data set was under the auspices of the modeling groups, the Program for Climate Model Diagnosis and Intercomparison (PCMDI) and the WCRP's Working Group on Coupled Modeling (WGCM). Support of this data set is provided by the Office of Science, U.S. Department of Energy. Macros for the graphical analysis and display of step changes were modified from those developed by D. Kelly O'Day.

References

- Alexandersson, H. (1986), A homogeneity test applied to precipitation data, *Int. J. Climatol.*, 6(6), 661–675, doi:10.1002/joc.3370060607.
- Brohan, P., J. J. Kennedy, I. Harris, S. F. B. Tett, and P. D. Jones (2006), Uncertainty estimates in regional and global observed temperature changes: A new data set from 1850, *J. Geophys. Res.*, 111, D12106, doi:10.1029/2005JD006548.

- Bücher, A., and J. Dessens (1991), Secular trend of surface temperature at an elevated observatory in the Pyrenees, *J. Clim.*, 4, 859–868, doi:10.1175/1520-0442(1991)004<0859:STOSTA>2.0.CO;2.
- Budyko, M. I. (1977), *Climatic Changes*, 261 pp., AGU, Washington, D. C., doi:10.1029/SP010.
- Bureau of Meteorology (2006), An exceptionally dry decade in parts of southern and eastern Australia: October 1996–September 2006, *Spec. Clim. Rep.*, 9, Melbourne, Victoria, Australia.
- Cai, W. J., and R. N. Jones (2005), Response of potential evaporation to climate variability and change: What GCMs simulate, paper presented at Pan Evaporation: An Example of the Detection and Attribution of Trends in Climate Variables, Aust. Acad. of Sci., Canberra, ACT, Australia.
- Chessman, B. C. (2009), Climatic changes and 13-year trends in stream macroinvertebrate assemblages in New South Wales, Australia, *Global Change Biol.*, 15, 2791–2802, doi:10.1111/j.1365-2486.2008.01840.x.
- Christidis, N., P. Stott, F. Zwiers, H. Shiogama, and T. Nozawa (2012), The contribution of anthropogenic forcings to regional changes in temperature during the last decade, *Clim. Dyn.*, doi:10.1007/s00382-011-1184-0, in press.
- Coughlan, M. J. (1979), Recent variations in annual-mean maximum temperatures over Australia, *Q. J. R. Meteorol. Soc.*, 105, 707–719, doi:10.1002/qj.49710544514.
- CSIRO and BoM (Eds.) (2007), Climate change in Australia, technical report, 148 pp., CSIRO, Melbourne, Victoria, Australia.
- Della-Marta, P. M., et al. (2004), Updating Australia's high-quality annual temperature dataset, *Aust. Meteorol. Mag.*, 53, 75–93.
- Dessai, S., et al. (2009), Climate prediction: A limit to adaptation?, in *Living With Climate Change: Are There Limits to Adaptation?*, edited by N. Adger et al., pp. 64–78, Cambridge Univ. Press, Cambridge.
- Douglass, D. H., and R. S. Knox (2009), Ocean heat content and Earth's radiation imbalance, *Phys. Lett. A*, 373(36), 3296–3300, doi:10.1016/j.physleta.2009.07.023.
- Douville, H. (2006), Detection-attribution of global warming at the regional scale: How to deal with precipitation variability?, *Geophys. Res. Lett.*, 33, L02701, doi:10.1029/2005GL024967.
- Easterling, D. R., and T. C. Peterson (1995), A new method for detecting undocumented discontinuities in climatological time series, *Int. J. Climatol.*, 15(4), 369–377, doi:10.1002/joc.3370150403.
- Evans, J. (2009), 21st century climate change in the Middle East, *Clim. Change*, 92(3–4), 417–432, doi:10.1007/s10584-008-9438-5.
- Fredriksen, J., et al. (2010), Causes of changing Southern Hemisphere weather systems, in *Managing Climate Change: Papers From the Greenhouse 2009 Conference*, edited by I. Jubb, P. Holper, and W. J. Cai, pp. 85–98, CSIRO Publ., Melbourne, Victoria, Australia.
- Gan, T. Y. (1995), Trends in air temperature and precipitation for Canada and North-eastern USA, *Int. J. Climatol.*, 15(10), 1115–1134, doi:10.1002/joc.3370151005.
- Granger, R. J. (1989), A complementary relationship approach for evaporation from nonsaturated surfaces, *J. Hydrol.*, 111(1–4), 31–38, doi:10.1016/0022-1694(89)90250-3.
- Hansen, J., R. Ruedy, J. Glascoe, and M. Sato (1999), GISS analysis of surface temperature change, *J. Geophys. Res.*, 104, 30,997–31,022, doi:10.1029/1999JD900835.
- Hansen, J., R. Ruedy, M. Sato, M. Imhoff, W. Lawrence, D. Easterling, T. Peterson, and T. Karl (2001), A closer look at United States and global surface temperature change, *J. Geophys. Res.*, 106, 23,947–23,963, doi:10.1029/2001JD000354.
- Hasselmann, K. (1979), On the signal-to-noise problem in atmospheric response studies, in *Meteorology of Tropical Oceans*, edited by D. B. Shaw, pp. 251–259, R. Meteorol. Soc., London.
- Hawkins, E., and R. Sutton (2011), The potential to narrow uncertainty in projections of regional precipitation change, *Clim. Dyn.*, 37(1–2), 407–418, doi:10.1007/s00382-010-0810-6.
- Hegerl, G. C., et al. (2010), Good practice guidance paper on detection and attribution related to anthropogenic climate change, in *Meeting Report of the Intergovernmental Panel on Climate Change Expert Meeting on Detection and Attribution of Anthropogenic Climate Change*, edited by T. F. Stocker et al., p. 8, IPCC Working Group I Tech. Support Unit, Univ. of Bern, Bern.
- Herweijer, C., et al. (2007), North American droughts of the last millennium from a gridded network of tree-ring data, *J. Clim.*, 20(7), 1353–1376, doi:10.1175/JCLI4042.1.
- Hope, P., et al. (2010), Associations between rainfall variability in the southwest and southeast of Australia and their evolution through time, *Int. J. Climatol.*, 30, 1360–1371.
- Hulme, M., and L. Mearns (2001), Climate scenario development, in *Climate Change 2001: The Scientific Basis 2001*, edited by J. T. Houghton et al., pp. 739–768, Cambridge Univ. Press, Cambridge, U. K.
- IPCC-TGICA (2007), General guidelines on the use of scenario data for climate impact and adaptation assessment: Version 2, report, 66 pp., Task Group on Scenarios for Clim. Impact Assess., Geneva, Switzerland.
- Jones, D., D. Collins, N. Nicholls, J. Phan, and P. Della-Marta (2004), A new tool for tracking Australia's climate variability and change, *Bull. Aust. Meteorol. Oceanogr. Soc.*, 17, 65–69.
- Jones, D. A., W. Wang, and R. Fawcett (2009), High-quality spatial climate data-sets for Australia, *Aust. Meteorol. Oceanogr. J.*, 58, 233–248.
- Jones, R. N. (2009), Assessment and review of Melbourne Water/CSIRO 2005 Climate Change Study projections, report, 23 pp., Cent. for Strategic Econ. Stud., Victoria Univ., Melbourne, Victoria, Australia.
- Jones, R. (2010a), A risk management approach to climate change adaptation, in *Climate Change Adaptation in New Zealand: Future Scenarios and Some Sectoral Perspectives*, edited by R. A. C. Nottage et al., pp. 10–25, New Zealand Clim. Change Cent., Wellington, New Zealand.
- Jones, R. N. (2010b), North central Victorian climate: Past, present and future, *Proc. R. Soc. Vic.*, 122(2), 147–160.
- Karoly, D. J., and K. Braganza (2005a), Attribution of recent temperature changes in the Australian region, *J. Clim.*, 18(3), 457–464, doi:10.1175/JCLI-3265.1.
- Karoly, D. J., and K. Braganza (2005b), A new approach to detection of anthropogenic temperature changes in the Australian region, *Meteorol. Atmos. Phys.*, 89(1–4), 57–67, doi:10.1007/s00703-005-0121-3.
- Kearney, M. R., et al. (2010), Early emergence in a butterfly causally linked to anthropogenic warming, *Biol. Lett.*, 6(5), 674–677, doi:10.1098/rsbl.2010.0053.
- Koster, R. D., et al. (2009), Analyzing the concurrence of meteorological droughts and warm periods, with implications for the determination of evaporative regime, *J. Clim.*, 22(12), 3331–3341, doi:10.1175/2008JCLI2718.1.
- Lettenmaier, D. P., E. F. Wood, and J. R. Wallis (1994), Hydro-climatological trends in the continental United States, 1948–88, *J. Clim.*, 7(4), 586–607.
- Li, F., et al. (2005), Relationships between rainfall in the southwest of Western Australia and near global patterns of sea-surface temperature and mean sea-level pressure variability, *Aust. Meteorol. Mag.*, 54, 23–33.
- MacCracken, M. C., et al. (2008), *Sudden and Disruptive Climate Change: Exploring the Real Risks and How We Can Avoid Them*, 326 pp., Earthscan, London.
- Mac Nally, R., et al. (2009a), Collapse of an avifauna: Climate change appears to exacerbate habitat loss and degradation, *Divers. Distrib.*, 15, 720–730, doi:10.1111/j.1472-4642.2009.00578.x.
- Mac Nally, R., et al. (2009b), Distribution of anuran amphibians in massively altered landscapes in south-eastern Australia: Effects in climate change in an aridifying region, *Global Ecol. Biogeogr.*, 18, 575–585, doi:10.1111/j.1466-8238.2009.00469.x.
- Madden, R. A., and J. Williams (1978), The correlation between temperature and precipitation in the United States and Europe, *Mon. Weather Rev.*, 106, 142–147, doi:10.1175/1520-0493(1978)106-0142:TCBTAP>2.0.CO;2.
- Maronna, R., and V. J. Yohai (1978), A bivariate test for the detection of a systematic change in mean, *J. Am. Stat. Assoc.*, 73(363), 640–645, doi:10.2307/2286616.
- Mayewski, P. A., et al. (2004), Holocene climate variability, *Quat. Res.*, 62(3), 243–255, doi:10.1016/j.yqres.2004.07.001.
- McDowall, D., et al. (1980), *Interrupted Time Series Analysis*, 97 pp., Sage, London.
- Meehl, G. A., et al. (2011), Model-based evidence of deep-ocean heat uptake during surface-temperature hiatus periods, *Nat. Clim. Change*, 1(7), 360–364, doi:10.1038/nclimate1229.
- Mitchell, T. D. (2003), Pattern scaling: An examination of the accuracy of the technique for describing future climates, *Clim. Change*, 60(3), 217–242, doi:10.1023/A:1026035305597.
- Murphy, B. F., and B. Timbal (2008), A review of recent climate variability and climate change in southeastern Australia, *Int. J. Climatol.*, 28(7), 859–879, doi:10.1002/joc.1627.
- Murphy, J., et al. (2009), Towards Prediction of Decadal Climate Variability and Change, paper presented at World Climate Conference - 3: Better Climate Information for a Better Future, World Meteorol. Org., Geneva, Switzerland.
- Nicholls, N. (2003), Continued anomalous warming in Australia, *Geophys. Res. Lett.*, 30(7), 1370, doi:10.1029/2003GL017037.
- Nicholls, N. (2010), Local and remote causes of the southern Australian autumn-winter rainfall decline, 1958–2007, *Clim. Dyn.*, 34(6), 835–845, doi:10.1007/s00382-009-0527-6.
- Nicholls, N., et al. (2004), 20th century changes in temperature and rainfall in New South Wales, *Aust. Meteorol. Mag.*, 53, 263–268.
- Overland, J., et al. (2008), North Pacific regime shifts: Definitions, issues and recent transitions, *Prog. Oceanogr.*, 77, 92–102, doi:10.1016/j.pocean.2008.03.016.

- Potter, K. (1981), Illustration of a new test for detecting a shift in mean in precipitation series, *Mon. Weather Rev.*, 109, 2040–2045, doi:10.1175/1520-0493(1981)109<2040:IOANTF>2.0.CO;2.
- Power, S., et al. (1998), Australian temperature, Australian rainfall, and the Southern Oscillation, 1910–1996: Coherent variability and recent changes, *Aust. Meteorol. Mag.*, 47, 85–101.
- Rodionov, S. N. (2005), A brief overview of the regime shift detection methods, in *Large-Scale Disturbances (Regime Shifts) and Recovery in Aquatic Ecosystems: Challenges for Management Toward Sustainability*. UNESCO-RÖSTE/BAS Workshop on Regime Shifts, edited by V. Velikova and N. Chipev, pp. 17–24, UNESCO, Varna, Bulgaria.
- Rodionov, S. N. (2006), Use of prewhitening in climate regime shift detection, *Geophys. Res. Lett.*, 33, L12707, doi:10.1029/2006GL025904.
- Santer, B. D., et al. (1990), Developing climate scenarios from equilibrium GCM results, report, 79 pp., Max Planck Inst. für Meteorol., Hamburg, Germany.
- Santer, B. D., et al. (2011), Separating signal and noise in atmospheric temperature changes: The importance of timescale, *J. Geophys. Res.*, 116, D22105, doi:10.1029/2011JD016263.
- Schneider, S. H. (2004), Abrupt non-linear climate change, irreversibility and surprise, *Global Environ. Change*, 14(3), 245–258, doi:10.1016/j.gloenvcha.2004.04.008.
- Stott, P. A., et al. (2010), Detection and attribution of climate change: A regional perspective, *Wiley Interdiscip. Rev. Clim. Change*, 1(2), 192–211.
- Swanson, K. L., and A. A. Tsonis (2009), Has the climate recently shifted?, *Geophys. Res. Lett.*, 36, L06711, doi:10.1029/2008GL037022.
- Swanson, K. L., et al. (2009), Long-term natural variability and 20th century climate change, *Proc. Natl. Acad. Sci. U. S. A.*, 106(38), 16,120–16,123, doi:10.1073/pnas.0908699106.
- Timbal, B. (2009), The continuing decline in south-east Australian rainfall —Update to May 2009, *CAWCR Res. Lett.*, 2, 4–11.
- Timbal, B., et al. (2010), Understanding the anthropogenic nature of the observed rainfall decline across south-eastern Australia, *CAWCR Tech. Rep.* 026, 180 pp., Cent. for Aust. Weather and Clim. Res., Melbourne, Victoria, Australia.
- Trenberth, K. E., and D. J. Shea (2005), Relationships between precipitation and surface temperature, *Geophys. Res. Lett.*, 32, L14703, doi:10.1029/2005GL022760.
- Ummenhofer, C. C., et al. (2009), What causes southeast Australia's worst droughts?, *Geophys. Res. Lett.*, 36, L04706, doi:10.1029/2008GL036801.
- Vivès, B., and R. N. Jones (2005), Detection of abrupt changes in Australian decadal rainfall (1890–1989), *CSIRO Atmos. Res. Tech. Pap.* 73, 54 pp., CSIRO, Melbourne, Victoria, Australia.
- Wanner, H., et al. (2008), Mid- to Late Holocene climate change: An overview, *Quat. Sci. Rev.*, 27(19–20), 1791–1828, doi:10.1016/j.quascirev.2008.06.013.
- Whetton, P. H., et al. (2005), Australian climate change projections for impact assessment and policy application: A review, *CSIRO Mar. Atmos. Res. Tech. Pap.* 1, 34 pp., CSIRO, Melbourne, Victoria, Australia.

R. N. Jones, Centre for Strategic Economic Studies, Victoria University, PO Box 14428, Melbourne, Vic 8001, Australia. (roger.jones@vu.edu.au)